PHILOSOPHICAL TRANSACTIONS OF THE ROYAL SOCIETY A MATHEMATICAL, PHYSICAL & ENGINEERING SCIENCES

Recent Advances in Studies of Carbon Fibre Structure [and Discussion]

D. J. Johnson and Charles Frank

Phil. Trans. R. Soc. Lond. A 1980 **294**, 443-449
doi: 10.1098/rsta.1980.0053

Phil. Trans. R. Soc. Lond. A **294**, 443–449 (1980)
Printed in Great Britain

Recent advances in studies of carbon fibre structure

By D. J. Johnson
Textile Physics Laboratory, Department of Textile Industries, University of Leeds, Leeds, LS2 9JT, U.K.

[Plates 1 and 2]

Carbon fibre structure is usually characterized by means of X-ray diffraction measurement and electron microscope observation. The meaning of the most important parameters is discussed in terms of the structures revealed by high resolution transmission electron microscopy. Recently, dark-field electron microscopy and electron diffraction of selected areas has been used to reveal and characterize skin–core and sheath–core heterogeneity in type I (2500 °C) polyacrylonitrile (PAN)-based carbon fibres. Lattice-fringe electron microscopy has given some insight into the nature of the surface layers in type I, type II (1500 °C) and type A (1000 °C) fibres. The skin regions of type I fibres are seen to contain misorientated crystallites interlinked in a complex manner; these are flaws that will limit the intrinsic tensile strength of the material.

Introduction

Carbon fibre structure has usually been characterized by means of quantitative wide-angle and small-angle X-ray diffraction methods supplemented by qualitative electron microscope investigations utilizing bright-field, dark-field, and lattice-imaging techniques. Detailed descriptions of X-ray and electron microscope methods and results from polyacrylonitrile (PAN)-based, cellulose-based, and pitch-based carbon fibres, are included in reviews by Johnson (1971), Fourdeux *et al.* (1971), and Reynolds (1973). The electron microscope evidence was obtained mainly from fibres heat treated to around 2500 °C and fragmented before examination; as a consequence, *in situ* studies were the province of light microscopy, scanning electron microscopy, and high voltage transmission electron microscopy. Recently, advances in sectioning techniques and improvements in the performance of transmission electron microscopes, have made it possible to observe lattice fringes in ultra-thin sections from carbon fibres heat treated not only at 2500 °C, but also at lower temperatures. Structural heterogeneity has been observed and quantitative estimations of characterization parameters are now possible from selected-area electron diffraction patterns.

X-ray diffraction

Wide angle parameters

Wide angle X-ray diffraction patterns for PAN-based type I (2500 °C) and type II (1500 °C) fibres are shown in figures 1 and 2 (plate 1). Type A fibres have a very similar pattern to that of type II fibres. The absence of *hkl* reflexions with $l > 0$ indicates a 'turbostratic' packing of graphitic layers with no regularity of packing in the *c*-axis direction. The main equatorial reflexion 002 comes from the layer planes spaced at about 0.34 nm ($c/2$); the half-height width,

or alternatively integral breadth, B_{002}, in the equatorial direction, is used to measure the stacking size L_c. $L_c = K\lambda/B_{002}\cos\theta$, where θ is the Bragg angle and λ the wavelength of radiation. K, the Scherrer parameter, can be considered as the factor by which the apparent size must be multiplied to give the true size, and for $00l$ reflexions is generally given the value of 0.89 for half width or 1.0 for integral breadth. A measure of lattice order can be obtained from a plot of integral breadth Δs against l for the $00l$ reflexions where

$$\Delta s = K/L_c + 2\pi^2\sigma^2 l^2,$$

$s = 2\sin\theta/\lambda$, σ is the r.m.s. local lattice disorder $\Delta d/d$, $d = \frac{1}{2}c$. The 100 reflexion is spread into a ring because of the turbostratic packing; the meridional width B_{100} gives a measure of layer-plane length $L_{a\parallel}$ parallel to the fibre axis; similarly, the equatorial width B_{100} is used to obtain the layer-plane dimension $L_{a\perp}$ perpendicular to the fibre axis, K values for $hk0$ reflexions (around 2.0) have been evaluated theoretically by Ruland & Tompa (1972) as a function of the preferred orientation parameter q.

The azimuthal spread of the 002 reflexion is due to a number of over-lapping diffraction arcs from misoriented crystallites. Intensity measurements in the aximuthal direction can be converted to a parameter q, which varies from $+1$ for perfect orientation perpendicular to the fibre axis, through 0 for random orientation, to -1 for perfect orientation parallel to the fibre axis (Ruland 1967). A simpler and more commonly used parameter for preferred orientation is Z, the half-height width of the azimuthal intensity distribution, which is a measure of the average misalignment of the basal planes to the fibre axis; i.e. the basal planes (layer planes) lie within $\frac{1}{2}Z°$ to either side of the fibre axis.

The main physical parameters for samples of type I, type II, and type A, PAN-based carbon fibres are given in table 1. Characterization parameters found by Oates (1974) are presented in table 2. The increasing values of L_c, $L_{a\parallel}$, and $L_{a\perp}$, and the decreasing value of Z with increasing heat-treatment temperature, correlate well with the increasing Young modulus. The decrease in strength in the high temperature material is usually attributed to the presence of gross flaws (Johnson & Thorne 1969); the intrinsic strength should be much higher. Moreton & Watt (1974) have shown that PAN precursor fibres made by careful filtration of the spinning solution before spinning into fibres in clean-room conditions gave carbon fibres, after treatment to 2500 °C, which did not show this drop in strength. Nevertheless, surface flaws, so far not characterized, are present, so that the fibre strengths are not greater than those of the fibres prepared at 1500 °C.

TABLE 1. PHYSICAL PROPERTIES OF PAN-BASED CARBON FIBRES

fibre	h.t.t./°C	Young modulus/(GN m^{-2})	tensile strength/(GN m^{-2})	density/(kg m^{-3})
type I	2500	390	2.2	1950
type II	1500	250	2.7	1750
type A	1000	210	2.7	1650

TABLE 2. STRUCTURAL PARAMETERS OF PAN-BASED CARBON FIBRES OBTAINED BY X-RAY DIFFRACTION

fibre	L_c/nm	$\frac{1}{2}c$/nm	σ/%	Z/deg	$-q$	$L_{a\parallel}$/nm	$L_{a\perp}$/nm	l_p/nm
type I	5.3	0.35	0.9	20	0.78	9.8	8.0	2.5
type II	1.7	0.36	—	41	0.55	3.9	2.7	1.4
type A	1.2	0.37	—	44	0.51	3.2	1.9	0.9

Small-angle parameters

Small-angle X-ray diffraction patterns for PAN-based type I (2500 °C) and type II (1500 °C) fibres are shown in figures 3 and 4 (plate 1); again the pattern for type A (1000 °C) fibres is very similar to that for type II fibres. It is generally assumed that the lobe-shaped pattern is due to needle-shaped pores or voids between crystallites. According to Porod's law, plots of Is^3 should reach a limiting value which, after appropriate correction, can be utilized to evaluate the pore-size parameter l_p (a distance of heterogeneity related to pore width), the crystallite-size parameter l_c, and S_v, the specific internal surface (Perret & Ruland 1968, 1969). An alternative method is to plot $I^{-\frac{1}{2}}$ against s^2 (or θ^2) for a fragmented specimen; if a straight line relation exists, the slope-to-intercept ratio can be used to yield a correlation length from which the small-angle parameters can be evaluated (Johnson & Tyson 1969, 1970). Values of l_p obtained by Oates (1974) following the latter method are included in table 2.

Electron microscopy

Interpretation of X-ray parameters

A study of high-resolution images showing the 0.34 nm lattice fringes from the (002) layer planes gives a good indication of the meaning and limitations of the X-ray parameters. Figure 5 (plate 1) taken from a fragment of a pitch-based carbon fibre heat treated to 2500 °C is an example. In terms of crystallite thickness there is clearly a size distribution of which L_c represents an average value. A detailed description of crystallite-size distributions and their measurement from various lattice-fringe images, and from X-ray and electron diffraction, has been reported by Bennett *et al.* (1976). In terms of layer-plane length, we can see that the actual length as observed in the lattice-fringe image is considerably greater than the X-ray diffraction value $L_{a_\parallel}$, which represents a coherence length related to the straight length of the layer planes. Similarly, $L_{a_\perp}$ represents the average straight dimension, i.e. width, of the layer plane at right angles to the fibre axis; transverse sections reveal considerable curvature of the layer planes in this direction and again the actual extent of the layer plane is much greater than that measured by the diffraction parameter.

The three dimensional complexity of the void system between crystallites in high temperature treated fibres can be seen clearly in figure 5 (plate 1), indeed the description of 'needle-shaped' voids seems reasonably accurate. Void structure in the lower temperature treated fibres is much more difficult to interpret, the small-angle scattering indicating that type II and type A fibres contain both density variations due to voids and density fluctuations due to stacking disorder (Perret & Ruland 1970); this high stacking disorder is also evident from the lack of high orders of $00l$ in the wide-angle diffraction pattern and the consequent impossibility of evaluating the lattice order parameter σ. A study of lattice-fringe images from sections of type II and type A fibres, figures 10 and 11 (plate 2) reveals obvious lattice disorder but no true voids. The distinction between a true void and a larger than normal layer spacing is apparently seen to best advantage in a fibre fragment, figure 6 (plate 1). However, this type of image must be interpreted with caution since information gaps in the phase-contrast transfer function at certain levels of focus can give an anomalous void-like appearance (Crawford & Marsh 1977).

PHILOSOPHICAL TRANSACTIONS OF THE ROYAL SOCIETY A MATHEMATICAL, PHYSICAL & ENGINEERING SCIENCES

Structural heterogeneity

It has been found that oxidation of the precursor fibres under tension is an essential stage in the production of carbon fibres from PAN (Watt 1970). Oxidation is either a reaction or a diffusion controlled process, depending upon such factors as the comonomers present in the PAN fibre, the temperature and time of oxidation, and the size and shape of the fibre cross section (Watt & Johnson 1975). The reaction controlled process produces uniform oxidation of the precursor fibre, the diffusion controlled process produces non-uniform oxidation and hence a two-zone structure in the oxidized fibre when the oxidation time has been insufficient. After heat treatment at 2500 °C observations in reflected polarized light of polished cross sections of carbon fibres made from fully stabilized PAN fibres† have been interpreted as revealing a uniform structure of circumferentially oriented layer planes. Similarly, cross sections of carbon fibres from understabilized PAN fibres suggested a two-zone or sheath–core structure where the outer zone, the sheath, appears to comprise circumferentially oriented layer planes, whereas the inner zone, the core, appears to be made up of radially oriented layer planes (Knibbs 1971; Wicks & Coyle 1976).

In order to clarify the optical-microscope characterization by electron microscope methods, particularly those of dark-field and lattice resolution, carbon fibres from circular section, commercially available, 1.5 and 3 denier, PAN fibres were prepared at R.A.E. Farnborough to show both two-zone and uniform cross sections in polarized light. Longitudinal and transverse sections were cut with an ultramicrotome and examined at Leeds in a Philips EM 300 electron microscope. Full details are published elsewhere (Bennett & Johnson 1979).

Longitudinal structure

All longitudinal sections of type I (2500 °C) carbon fibres, irrespective of denier or time of oxidation at 220 °C showed a uniform structure, apart from a thin skin between 150 and 250 nm in thickness. A typical example of this thin skin is illustrated in the 002 dark-field image of figure 7 (plate 1). There was no evidence in type I carbon fibres from fully stabilized PAN for circumferentially oriented layer planes in the core, nor was there evidence in type I

† Fully stabilized PAN fibres are fibres that have been oxidized under conditions of time and temperature such that no sheath–core structure is visible in the oxidized fibres, and the uptake of oxygen is greater than 6% by mass.

Description of plate 1

Figure 1. Wide-angle X-ray diffraction pattern of PAN-based type I (2500 °C) carbon fibre.

Figure 2. Wide-angle X-ray diffraction pattern of PAN-based type II (1500 °C) carbon fibre.

Figure 3. Small-angle X-ray diffraction pattern of PAN-based type I (2500 °C) carbon fibre.

Figure 4. Small-angle X-ray diffraction pattern of PAN-based type II (1500 °C) carbon fibre.

Figure 5. Lattice-fringe image from a fragment of pitch-based (2500 °C) carbon fibre, indicating the interpretation of typical characterization parameters.

Figure 6. Lattice-fringe image from a fragment of PAN-based type II (1500 °C) carbon fibre, illustrating voids and layer plane disorder.

Figure 7. Dark-field (002) image from longitudinal section of PAN-based type I (2500 °C) carbon fibre showing skin–core heterogeneity. Electron diffraction patterns of each region are inset.

Figure 8. Dark-field (002) image from longitudinal section of PAN-based type I (2500 °C) carbon fibre pre-vacuum treated for 6 h at 230 °C followed by oxidation in air for 1 h at 230 °C. Sheath–core heterogeneity is illustrated.

PHILOSOPHICAL TRANSACTIONS OF THE ROYAL SOCIETY A MATHEMATICAL, PHYSICAL & ENGINEERING SCIENCES

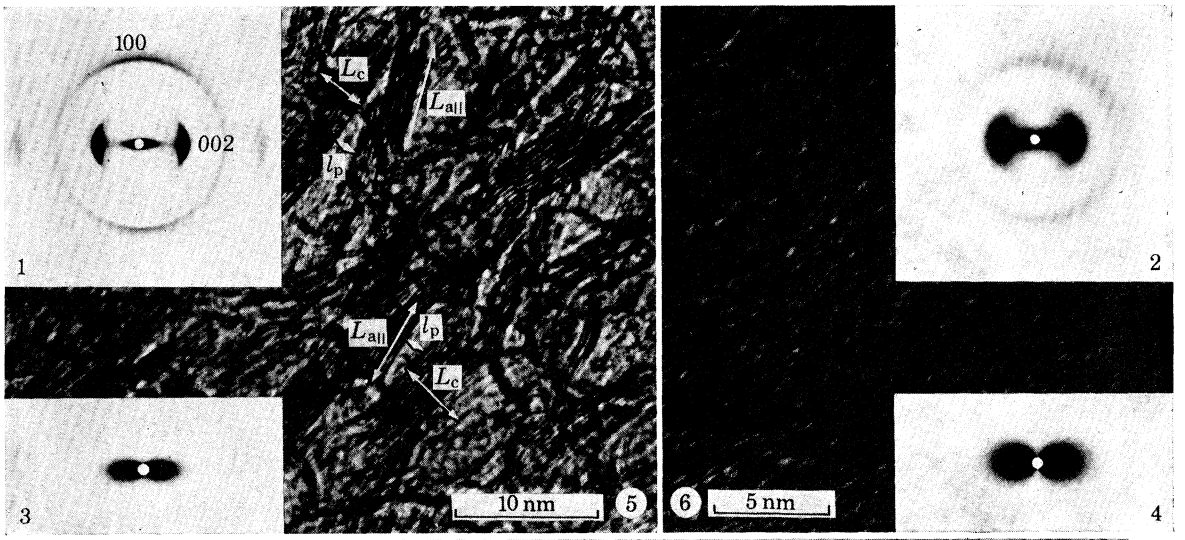

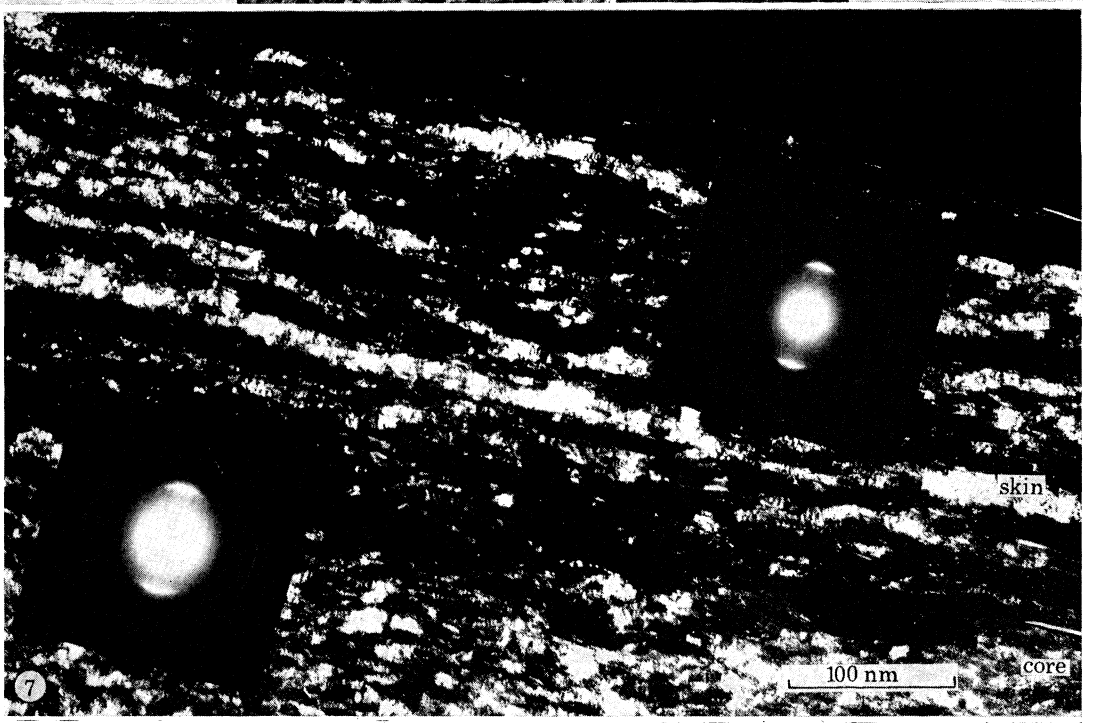

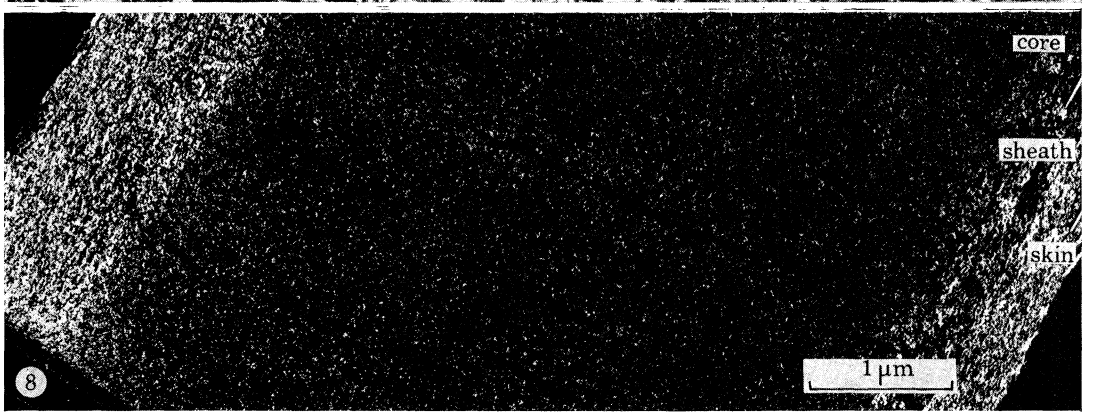

FIGURES 1–8. For description see opposite.

(*Facing p.* 446)

PHILOSOPHICAL TRANSACTIONS OF THE ROYAL SOCIETY A MATHEMATICAL, PHYSICAL & ENGINEERING SCIENCES

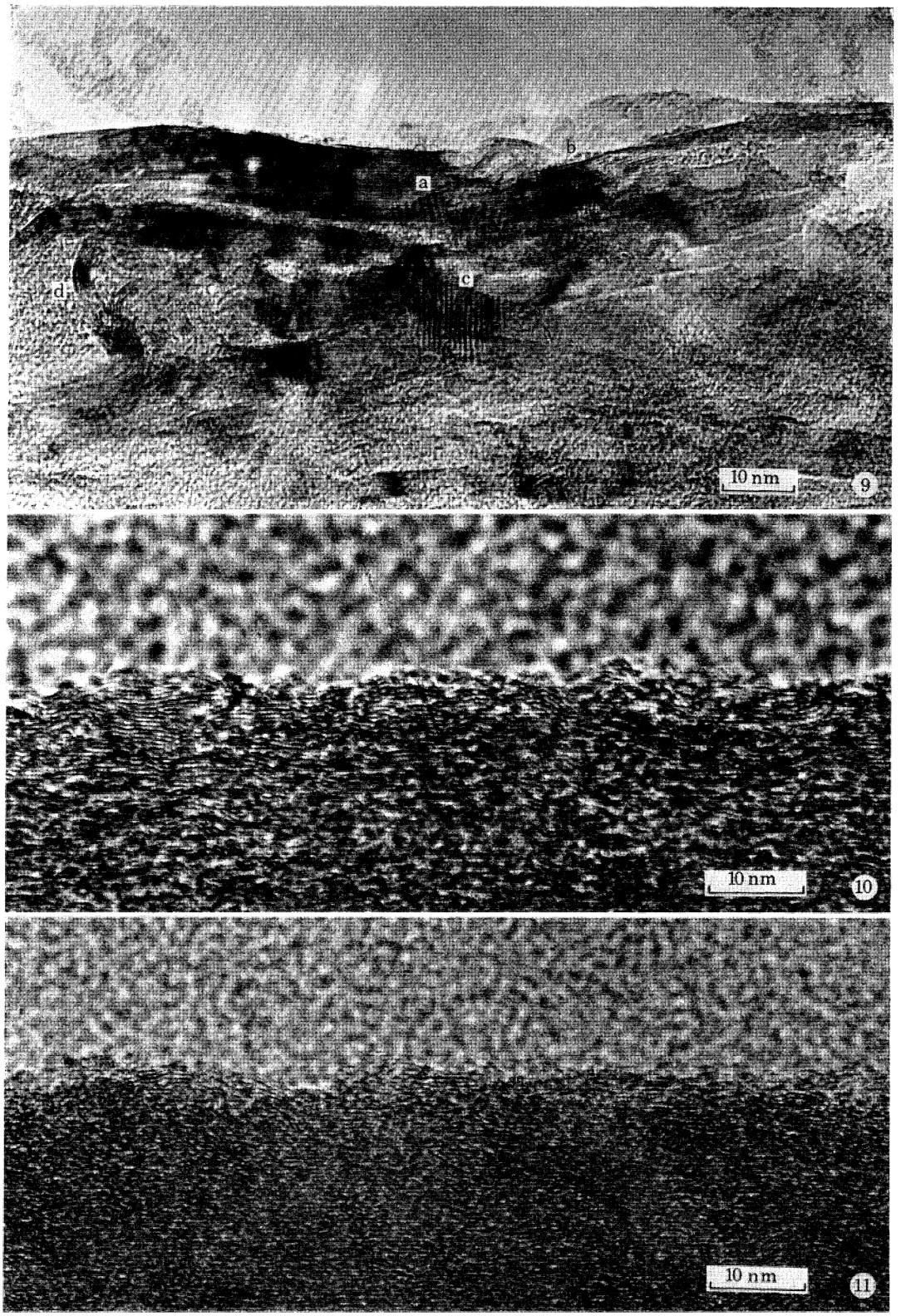

FIGURES 9–11. For description see opposite.

PHILOSOPHICAL TRANSACTIONS OF THE ROYAL SOCIETY A MATHEMATICAL, PHYSICAL & ENGINEERING SCIENCES

carbon fibres from understabilized PAN of the sheath–core structure observed with polarized light.

Electron diffraction patterns of skin and core regions, as inset, were analysed by means of a microdensitometer and a computational procedure for profile resolution (Bennett *et al.* 1974), which is essential for closely overlapping asymmetric peaks such as 100 and 004 on the equator. The skin was found to have a high axial preferred orientation, $Z = 14°$, and relatively thick crystallites, $L_c = 10.0$ nm; the core has a lower preferred orientation, $Z = 26°$, and thinner crystallites, $L_c = 3.3$ nm. Further parameters are given in table 3. A full characterization of the core structure, including the distribution of crystallite size with azimuthal angle is given in the paper by Bennett *et al.* (1976).

Transverse structure

Transverse sections of type I fibres from fully stabilized PAN fibres also show evidence of a thin skin in both dark-field and lattice-fringe modes. This skin is seen to contain circumferentially arranged crystallites, but there is no evidence for any preferred organization in the core, which comprises 95% of the cross-sectional area. This randomly organized structure normal to the fibre axis for the bulk of the type I carbon fibre from fully stabilized PAN fibre is at variance with the circumferentially arranged structure suggested earlier from the observations with reflected polarized light. No quantitative or qualitative evidence for structural heterogeneity or preferred crystallite organization could be found in type II or type A fibres from fully stabilized PAN fibres.

TABLE 3. STRUCTURAL PARAMETERS OBTAINED BY ELECTRON DIFFRACTION OF CARBON FIBRES PREPARED FROM FULLY STABILIZED PAN FIBRES

fibre	region	L_c/nm	$\frac{1}{2}c$/nm	σ/%	Z/deg	$L_{a\parallel}$/nm	$L_{a\perp}$/nm
type I	skin	10.0	0.35	0.6	14	10.3	8.4
h.t.t. 2500 °C	core	3.3	0.35	1.5	26	7.4	4.8
type II	surface	1.6	0.35	—	43	—	—
h.t.t. 1500 °C	core	1.6	0.35	—	44	—	—
type A	surface	1.2	0.37	—	43	—	—
h.t.t. 1000 °C	core	1.2	0.37	—	43	—	—

When type I carbon fibres prepared from PAN fibres which had received a non-uniform oxidation treatment of 6 h in a vacuum at 230 °C followed by $\frac{1}{2}$ h in air at 230 °C, were examined, sheath–core heterogeneity was found in both longitudinal and transverse sections. A typical example is illustrated in the 002 dark-field image of figure 8 (plate 1). The sheath is around 1 μm in thickness and appears to be more crystalline than the core; a highly crystalline skin is also present at the surface of the fibre. Lattice-fringe images from sheath and core

---

DESCRIPTION OF PLATE 2

FIGURE 9. Lattice-fringe image from longitudinal section of PAN-based type I (2500 °C) carbon fibre, showing surface layers and misoriented crystallites in the skin.

FIGURE 10. Lattice-fringe image from longitudinal section of PAN-based type II (1500 °C) carbon fibre surface layers.

FIGURE 11. Lattice-fringe image from longitudinal section of PAN-based type A (1000 °C) carbon fibre, surface layers.

PHILOSOPHICAL TRANSACTIONS OF THE ROYAL SOCIETY A MATHEMATICAL, PHYSICAL & ENGINEERING SCIENCES

are very similar in longitudinal section; however, in transverse section, the layer planes in the sheath are seen to be more extensive than those in the core. There was no evidence for sheath–core heterogeneity in a specimen oxidized under uniform oxidation conditions.

Watt & Johnson (1975) have reported that the sheath region in the prevacuum treated specimen is oxygen rich; thus, lateral organization of the ladder polymer is enhanced and its subsequent conversion to layer planes at 2500 °C results in more extensive sheets than in the core. All the electron microscope evidence shows that both sheath and core regions have a random organization of the crystallites in the transverse structure; again this is contrary to the evidence from polarized light microscopy, so that another explanation is necessary to explain the polarized light observations.

Surface layers

The structure of the surface layers of carbon fibres is of considerable technological importance. Although the skin region of type I fibres contains layer planes oriented predominantly parallel to the surface, there are some crystallites, and hence layer planes, which are misoriented with respect to the fibre axis. Figure 9 (plate 2) contains some typical examples; at *a*, *b*, and *c*, sets of layer planes cross at angles of about 20°, 45°, and 30°, respectively, giving rise to Moiré fringes. At *d* a set of layer planes links two crystallites via an 'S' type bridge. These misoriented crystallites could well be the intrinsic flaws suggested by Reynolds & Sharp (1974) as strength limiting features in regions where gross flaws are absent. The distribution of misoriented crystallites in the core region has been described by Bennett *et al.* (1976).

Electron-microscope investigations of longitudinal sections of type II (1500 °C) and type A (1000 °C) carbon fibres from fully stabilized PAN fibres have shown no evidence for skin–core heterogeneity; this is confirmed by quantitative electron diffraction analysis, which cannot differentiate the region near the surface and that towards the interior (see table 3). Lattice-fringe images of the surface, as seen in longitudinal section, are depicted for type II fibres in figure 10 (plate 2) and for type A fibres in figure 11 (plate 2). Those few layers that form the surface itself are necessarily better oriented than those layers further away from the surface, but cannot be considered as a skin. Essentially the electron micrographs reveal the high stacking disorder characteristic of type II and type A fibres.

Conclusion

X-ray diffraction will continue to be a useful tool for routine structural characterization of carbon fibres. However, the techniques of dark- and bright-field transmission electron microscopy, together with lattice-fringe imaging and quantitative electron diffraction analysis, combine to give a much clearer insight into the structure of carbon fibres, particularly where structural heterogeneity must be characterized, or where the physical nature of the surface layers is under investigation.

I wish to thank my former research students, C. N. Tyson, C. Oates, D. Crawford and S. C. Bennett, for their invaluable work on the structural characterization of PAN-based carbon fibres. I am indebted to W. Johnson and W. Watt of the Royal Aircraft Establishment, who instituted the investigation of sheath–core heterogeneity, provided specimens, helped with section cutting, and participated in many informative discussions. Thanks are also due to the Ministry of Defence, Procurement Executive, for financial assistance.

PHILOSOPHICAL TRANSACTIONS OF THE ROYAL SOCIETY A MATHEMATICAL, PHYSICAL & ENGINEERING SCIENCES

References (Johnson)

Bennett, S. C. & Johnson, D. J. 1979 *Carbon* **17**, 25–39.
Bennett, S. C., Johnson, D. J. & Montague, P. E. 1974 *Fourth London Int. Conf. Carbon and Graphite*, pp. 503–507. London: Society of Chemical Industry.
Bennett, S. C., Johnson, D. J. & Murray, R. 1976 *Carbon* **14**, 117–122.
Crawford, D. & Marsh, H. 1977 *J. Microsc.* **109**, 145–152.
Fourdeux, A., Perret, R. & Ruland, W. 1971 *Proc. First Int. Conf. Carbon Fibres*, pp. 57–67. London: Plastics Institute.
Johnson, D. J. 1971 *Proc. First Inst. Conf. Carbon Fibres*, pp. 52–56. London: Plastics Institute.
Johnson, D. J. & Tyson, C. N. 1969 *J. Phys.* D **2**, 787–795.
Johnson, D. J. & Tyson, C. N. 1970 *J. Phys.* D **3**, 526–534.
Johnson, J. W. & Thorne, D. J. 1969 *Carbon* **7**, 659–661.
Knibbs, R. H. 1971 *J. Microsc.* **94**, 273–281.
Moreton, R. & Watt, W. 1974 *Nature, Lond.* **247**, 360.
Oates, C. D. 1974 Ph.D. Thesis. University of Leeds.
Perret, R. & Ruland, W. 1968 *J. appl. Crystallogr.* **1**, 308–313.
Perret, R. & Ruland, W. 1969 *J. appl. Crystallogr.* **2**, 209–218.
Perret, R. & Ruland, W. 1970 *J. appl. Crystallogr.* **3**, 525–532.
Reynolds, W. N. 1973 *Chem. Phys. Carbon* **11**, 1–67.
Reynolds, W. N. & Sharp, J. V. 1974 *Carbon* **12**, 103–110.
Ruland, W. 1967 *J. appl. Phys.* **38**, 3585–3589.
Ruland, W. & Tompa, H. 1972 *J. appl. Crystallogr.* **5**, 225–230.
Watt, W. 1970 *Proc. R. Soc. Lond.* A **319**, 5–15.
Watt, W. & Johnson, W. 1975 *Nature, Lond.* **257**, 210–212.
Wicks, B. J. & Coyle, R. A. 1976 *J. Mater. Sci.* **11**, 376–383.

Discussion

Sir Charles Frank, F.R.S. (*The H. H. Wills Physics Laboratory, Royal Fort, Bristol BS8 1TL, U.K.*). Dr Johnson told us that the small-angle X-ray scattering corresponds to disks in reciprocal space and is attributed to needle-shaped voids orientated more or less along the fibre direction. Then he showed us a model, due, I think, to Crawford, in which gaps appeared between warped stacks of lamellae, lamellae in these stacks being more or less parallel to the fibre axis, and the curvature shown being about a transverse axis. Would not this model rather indicate leaf-shaped or pancake-shaped rather than needle-shaped voids? The main axially orientated disclinations seen in some other models presented (which I believe to be essentially correct) would correspond to axially oriented needle-shaped regions of lower density (rather than voids) which could explain the observations.

D. J. Johnson. The Crawford model was intended to illustrate the three dimensional representation of the crystallite interlinking as seen in the lattice-fringe electron micrographs (see figure 5). While the description 'needle-shaped' is indeed adequate for a simple model, the three dimensional voids in type I fibres must have complex shapes which are not adequately described by any of the conventional terms for solids. Quantitative analysis (see Perret & Ruland 1970) indicates that type I fibres have small-angle X-ray scattering due to a crystallite–void system, but type II fibres have, in addition, scattering due to density fluctuations. The lattice-fringe images of type II fibres (see figure 6) indicate that these density variations are due to fluctuations in the interlayer spacing.

PHILOSOPHICAL TRANSACTIONS OF THE ROYAL SOCIETY A MATHEMATICAL, PHYSICAL & ENGINEERING SCIENCES

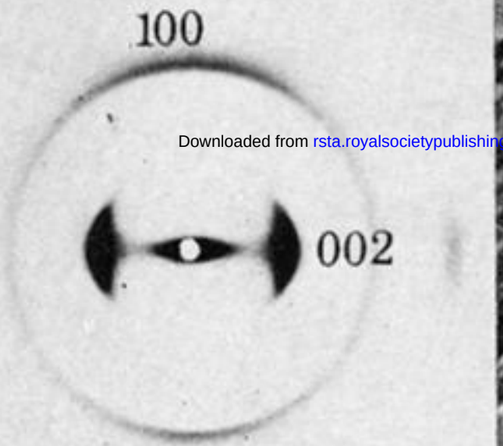

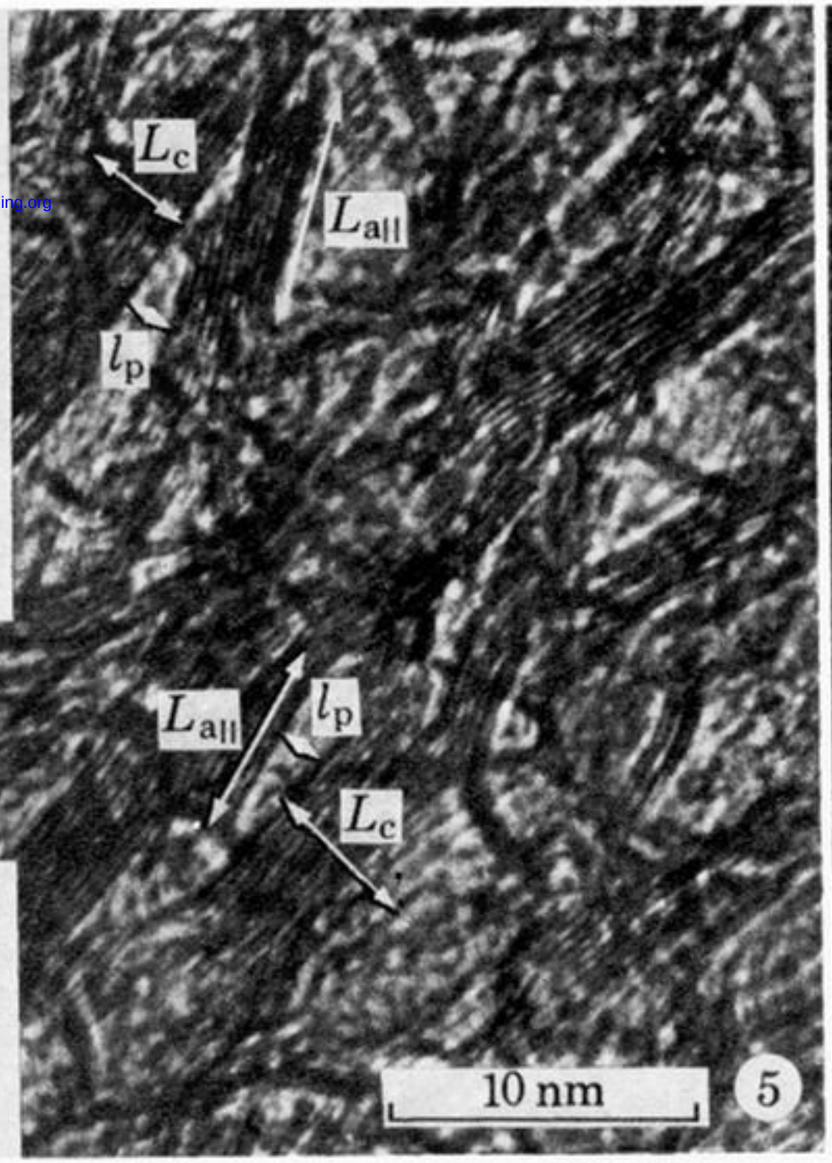

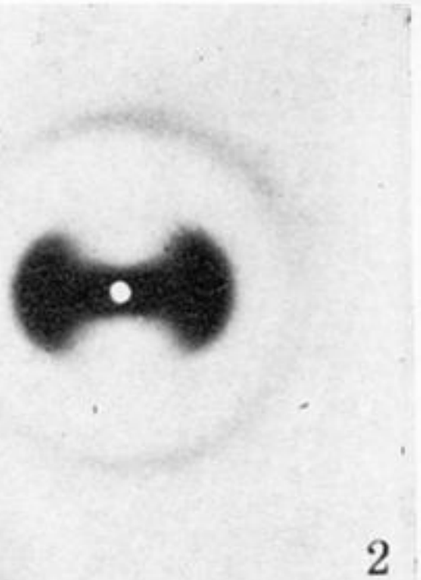

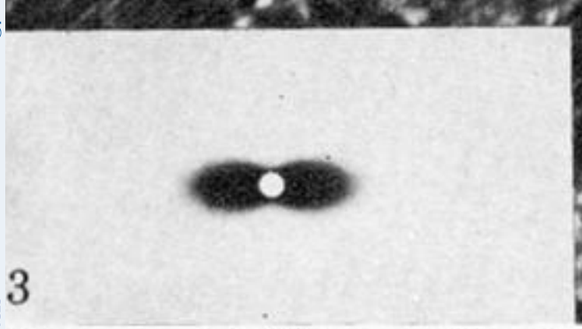

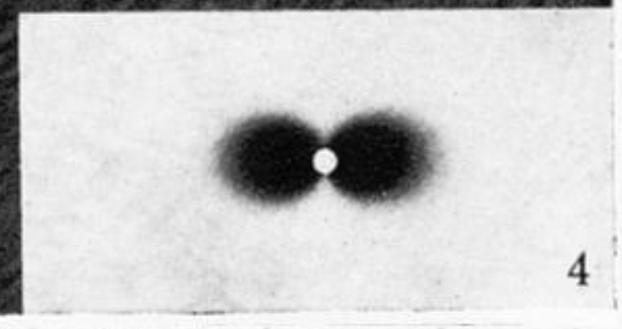

FIGURE 1. Wide-angle X-ray diffraction pattern of PAN-based type I (2500 °C) carbon fibre.

FIGURE 2. Wide-angle X-ray diffraction pattern of PAN-based type II (1500 °C) carbon fibre.

FIGURE 3. Small-angle X-ray diffraction pattern of PAN-based type I (2500 °C) carbon fibre.

FIGURE 4. Small-angle X-ray diffraction pattern of PAN-based type II (1500 °C) carbon fibre.

FIGURE 5. Lattice-fringe image from a fragment of pitch-based (2500 °C) carbon fibre, indicating the interpretation of typical characterization parameters.

FIGURE 6. Lattice-fringe image from a fragment of PAN-based type II (1500 °C) carbon fibre, illustrating voids and layer plane disorder.

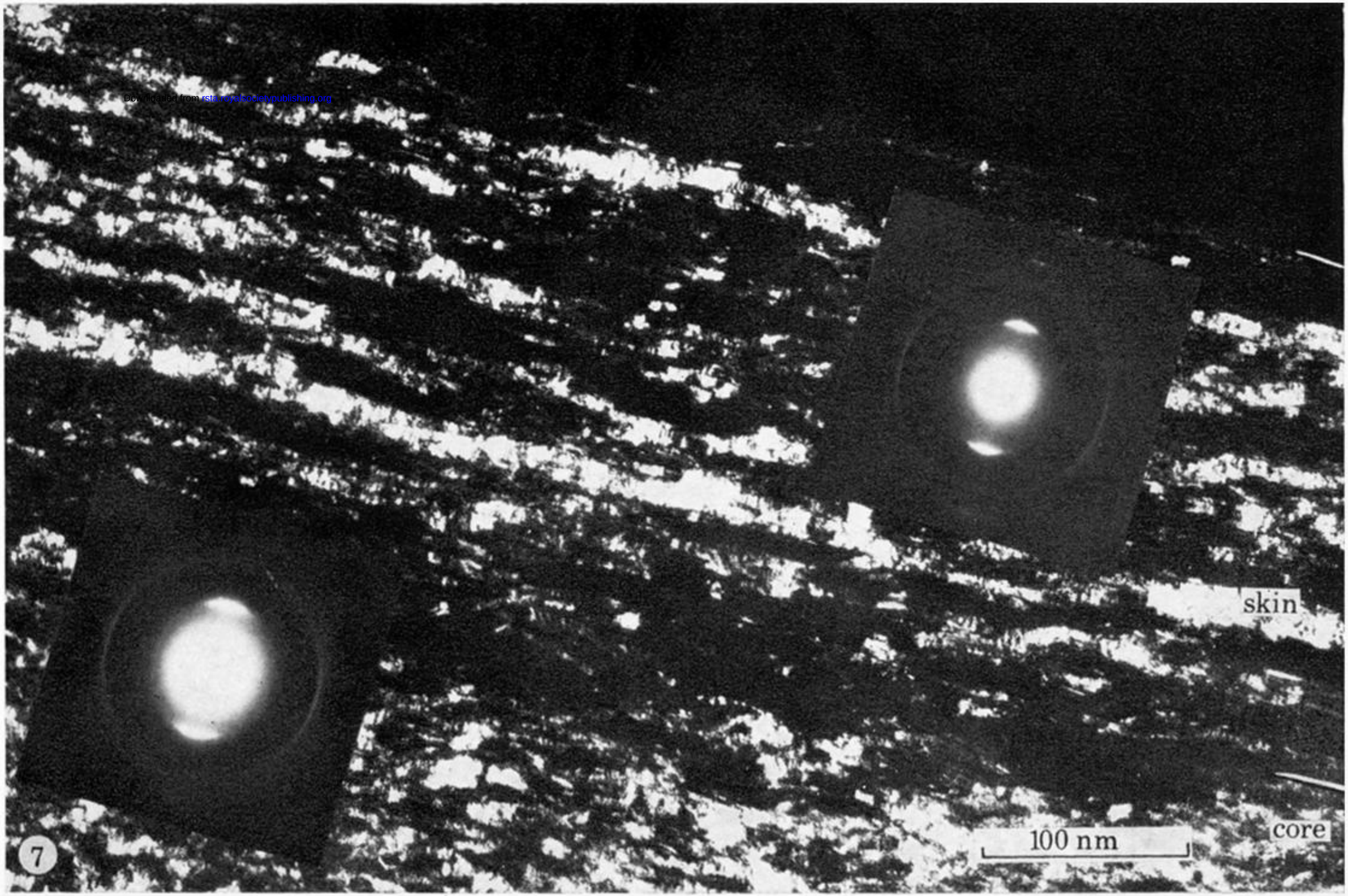

FIGURE 7. Dark-field (002) image from longitudinal section of PAN-based type I (2500 °C) carbon fibre showing skin–core heterogeneity. Electron diffraction patterns of each region are inset.

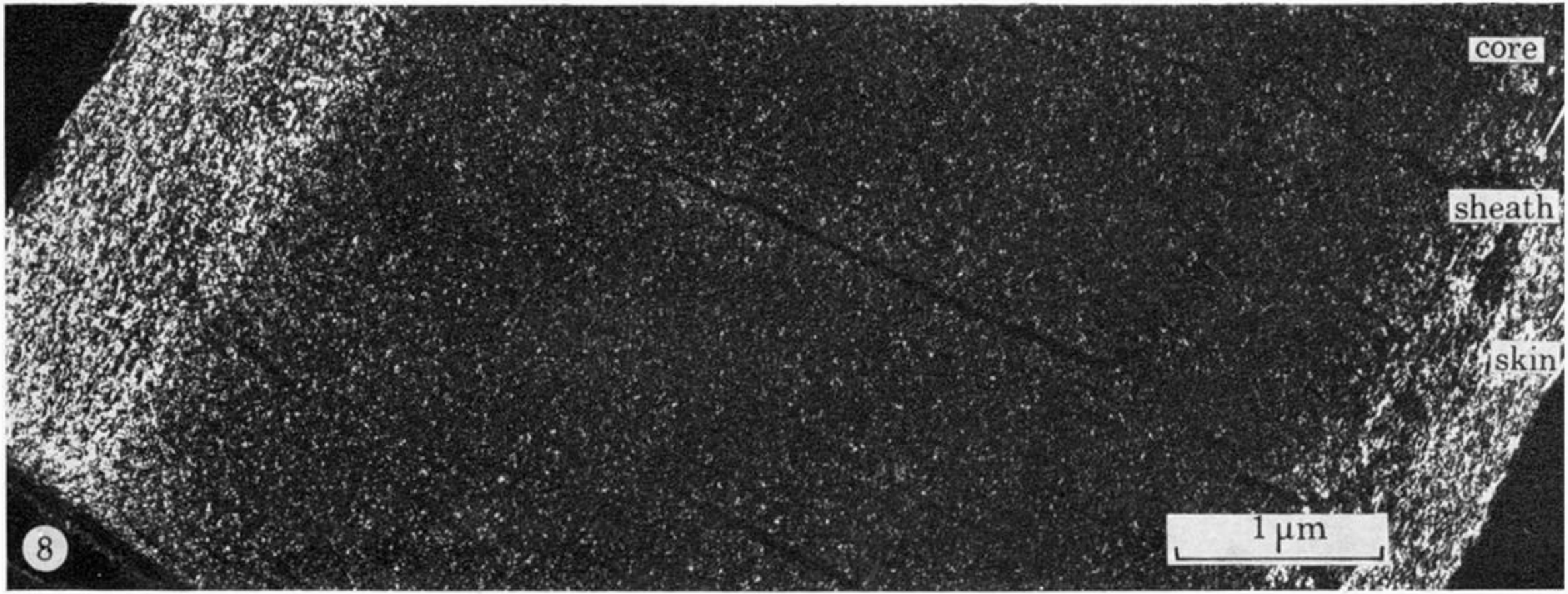

FIGURE 8. Dark-field (002) image from longitudinal section of PAN-based type I (2500 °C) carbon fibre pre-vacuum treated for 6 h at 230 °C followed by oxidation in air for 1 h at 230 °C. Sheath–core heterogeneity is illustrated.

FIGURE 9. Lattice-fringe image from longitudinal section of PAN-based type I (2500 °C) carbon fibre, showing surface layers and misoriented crystallites in the skin.

PHILOSOPHICAL TRANSACTIONS OF THE ROYAL SOCIETY A MATHEMATICAL, PHYSICAL & ENGINEERING SCIENCES

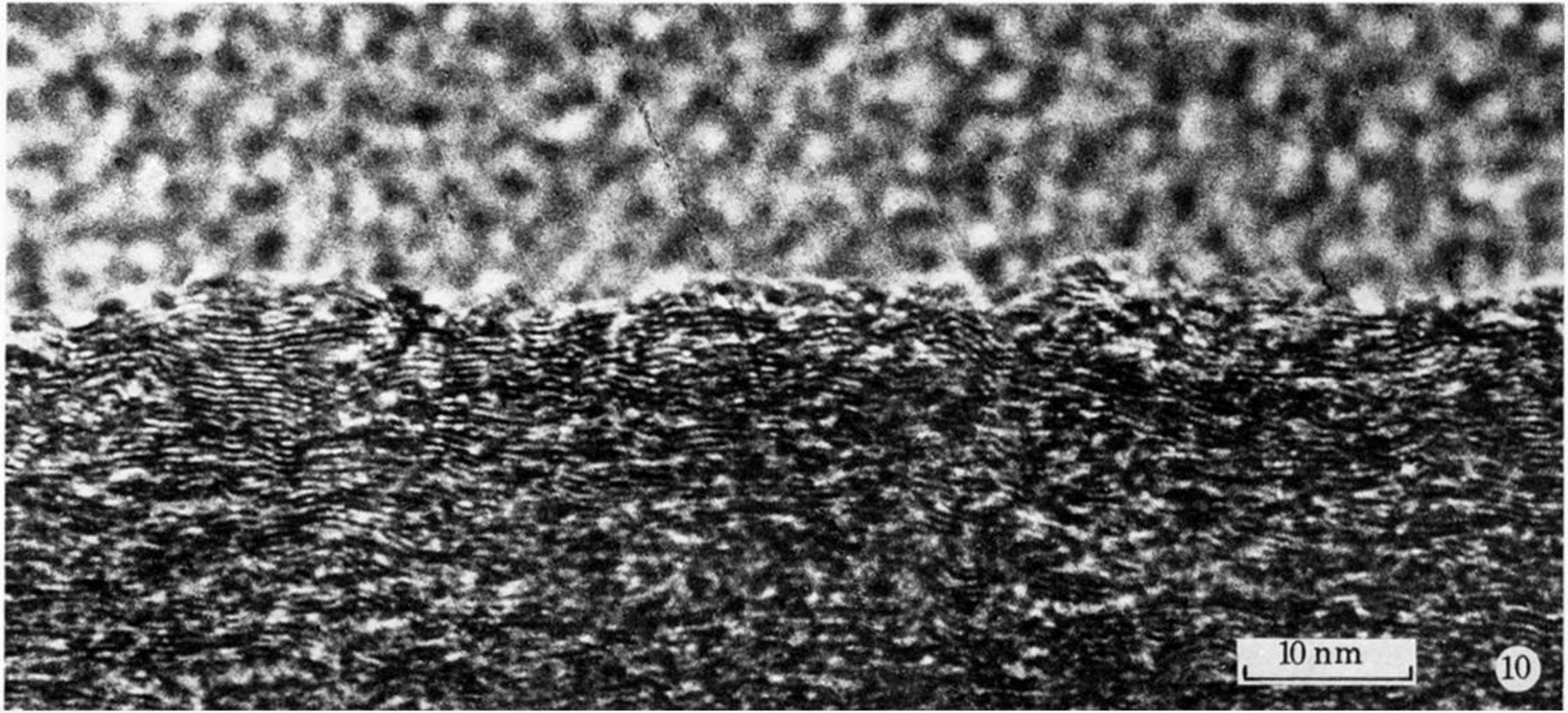

FIGURE 10. Lattice-fringe image from longitudinal section of PAN-based type II (1500 °C) carbon fibre surface layers.

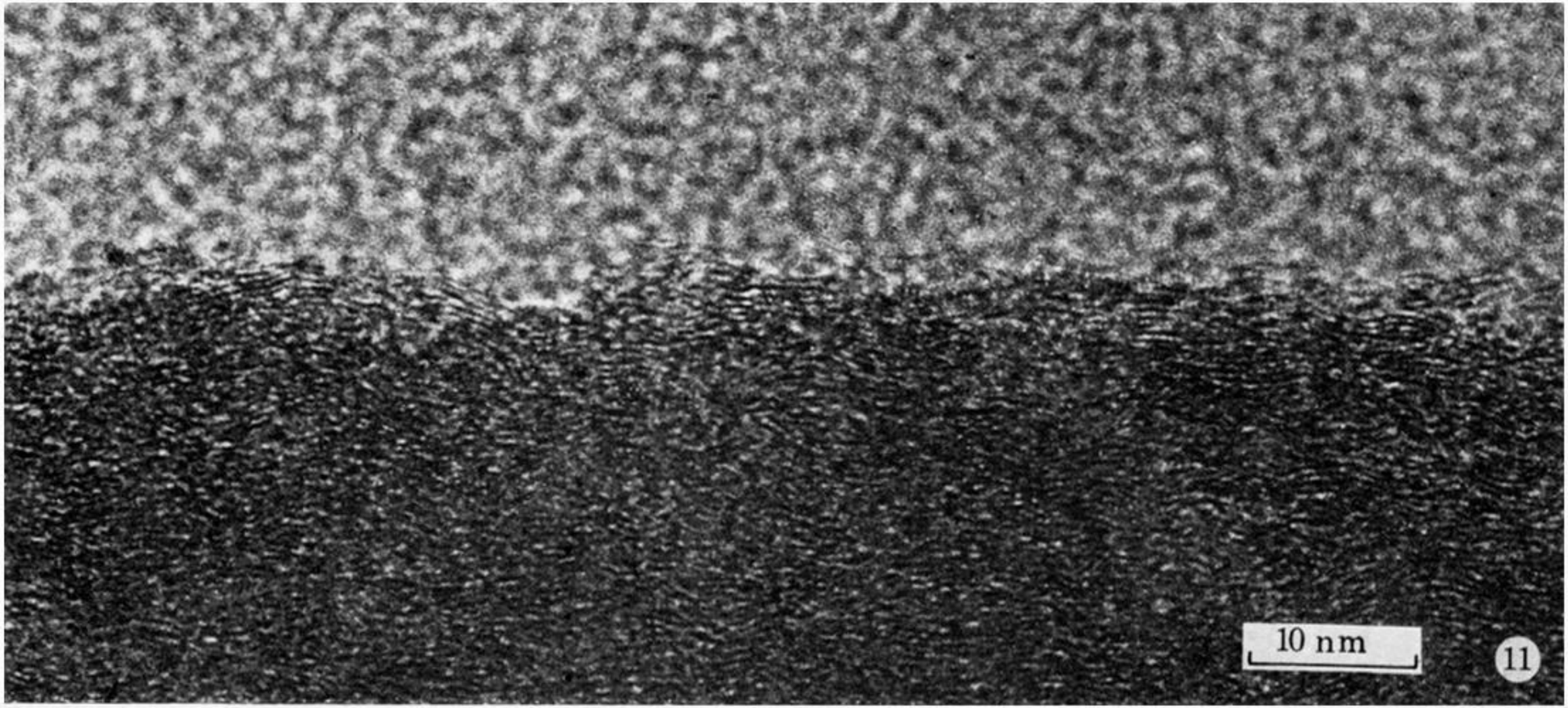

FIGURE 11. Lattice-fringe image from longitudinal section of PAN-based type A (1000 °C) carbon fibre, surface layers.

PHILOSOPHICAL TRANSACTIONS OF THE ROYAL SOCIETY A MATHEMATICAL, PHYSICAL & ENGINEERING SCIENCES